






Original Research

A Highly Selective and Sensitive Fluorescent Probe With a Large Stokes Shift for Near-Infrared Visualization of Endogenous and Exogenous Biothiols in Living Cells

Xiaomin Li¹, Rongrong Yuan¹, Yangmin Ma¹, Guanglong Li¹, Siyue Ma^{1,*}

¹Shaanxi Key Laboratory of Chemical Additives for Industry, College of Chemistry and Chemical Engineering, Shaanxi University of Science & Technology, 710021 Xi'an, Shaanxi, China

*Correspondence: masiyue@sust.edu.cn (Siyue Ma)

Academic Editor: Haseeb Ahmad Khan

Submitted: 16 January 2025 Revised: 12 March 2025 Accepted: 14 April 2025 Published: 23 May 2025

Abstract

Background: Fluorescent probes have become a powerful tool for monitoring biothiol concentrations, aiding in disease diagnosis and treatment while also facilitating the exploration of fundamental biological processes. However, the probes are limited by the short fluorescence emission wavelength and small Stokes shift, which makes them susceptible to background fluorescence interference and significant self-absorption. To overcome these limitations and achieve high-fidelity biothiols detection in complex biological systems, this study focuses on developing a near-infrared fluorescent probe with an extended Stokes shift. **Methods:** (E)-4-(5-(2-(4-(dicyanomethylene)-4H-chromen-2-yl)vinyl)thiophen-2-yl)phenyl 2,4-dinitrobenzenesulfonate (**DCMOS-N**), a near-infrared (NIR) fluorescent probe featuring a large Stokes shift, was designed and synthesized for biothiols detection. The optical properties of **DCMOS-N** were evaluated using ultraviolet-visible (UV-Vis) and fluorescence spectroscopy. Additionally, its imaging capabilities for detecting biothiols in living cells were assessed through confocal fluorescence microscopy. **Results:** Fluorescence spectral analysis confirmed that the **DCMOS-N** probe exhibits high selectivity and strong anti-interference properties in biothiol detection. Moreover, its fluorescence intensity increases upon the addition of biothiols. Notably, a strong linear correlation was observed across the concentration range of 0 to 100 $\mu\text{mol/L}$ ($R^2 = 0.9944$ for glutathione (GSH), 0.9942 for cysteine (Cys), and 0.9946 for homocysteine (Hcy)), enabling the quantitative analysis of biothiol concentrations in biological systems. The detection limits for GSH, Cys, and Hcy were determined as 0.142 $\mu\text{mol/L}$, 0.129 $\mu\text{mol/L}$, and 0.143 $\mu\text{mol/L}$, respectively. Importantly, the practical application of **DCMOS-N** in living cells was validated, with confocal fluorescence imaging demonstrating its capability to detect both endogenous and exogenous biothiols in HeLa cells. **Conclusion:** An NIR fluorescent probe, **DCMOS-N**, was developed and effectively utilized to monitor biothiols in living HeLa cells. The successful design of **DCMOS-N** presents significant potential and serves as an innovative platform for developing fluorescence probes targeted at biothiols.

Keywords: fluorescent probe; near-infrared fluorescence imaging; biothiols; large Stokes shifts

1. Introduction

Real-time monitoring of live cells is essential for diagnosing and treating diseases and exploring fundamental biological processes [1]. Fluorescent probes offer significant advantages owing to their non-invasive nature, high sensitivity, and specificity, enabling continuous, real-time tracking and visualization of cellular components [2–4]. However, the short fluorescence emission wavelength and small Stokes shift of the probes make them prone to interference from background fluorescence and significant self-absorption. To address these issues, near-infrared (NIR, 650–900 nm) fluorescent probes are particularly beneficial for biological imaging [5,6]. They provide deeper tissue penetration, reduce light scattering and absorption, and minimize background autofluorescence, thereby enhancing the detection of endogenous analytes in living cells [7–10].

Biothiols such as glutathione (GSH), cysteine (Cys), and homocysteine (Hcy) play a crucial role in maintaining human health [11]. Increasing evidence suggests that im-

balances in these biothiol levels can lead to severe health conditions, including cancer, cardiovascular diseases, neurological disorders, and metabolic dysfunctions [12–14]. Therefore, developing an NIR fluorescent probe to monitor biothiol fluctuations in living organisms could aid in early disease diagnosis and provide deeper insights into their pathological processes [15]. Recently, significant progress has been made in designing NIR probes specifically for biothiol detection [16–19]. However, most efforts have focused on the selective detection of only one or two of these biothiols. Given that multiple molecular events often occur simultaneously in the signal transduction pathways of living systems, there is a critical need for methods capable of detecting multiple biothiols concurrently across various disease stages.

The 2,4-dinitrobenzenesulfonyl (DNBS) group is widely recognized for its high selectivity, sensitivity, rapid response, and excellent biocompatibility in the design of fluorescent probes, making it a powerful tool for both biomedical research and clinical diagnostics



(Fig. 1a) [20]. Building on this concept, we developed a near-infrared (NIR) fluorescent probe, (E)-4-(5-(2-(4-(dicyanomethylene)-4H-chromen-2-yl)vinyl)thiophen-2-yl)phenyl 2,4-dinitrobenzenesulfonate (**DCMOS-N**) (Fig. 1b). This probe integrates a dicyanomethylene-4H-pyran (DCM) derivative as the fluorophore, which emits in the NIR spectrum, and employs the DNBS group for functional recognition. **DCMOS-N** exhibited a rapid NIR fluorescence turn-on response at 651 nm, with a substantial Stokes shift of 156 nm, along with exceptional sensitivity and selectivity for biothiols, free from interference by other potential analytes. Furthermore, **DCMOS-N** has been successfully utilized to detect both endogenous and exogenous biothiols in living cells.

2. Experimental Section

2.1 General Information

All reagents were obtained from commercial suppliers and were used and stored according to the manufacturer's specifications. Specifically, 5-Bromothiophene-2-Carbaldehyde (Catalog No. B801990), 4-Hydroxyphenylboronic Acid (Catalog No. H804864), Tetrakis (triphenylphosphine) palladium (Catalog No. T819527), 2,4-Dinitrobenzenesulfonyl Chloride (Catalog No. D830587), dimethyl sulfoxide (Catalog No. D806645), and deuterated dimethyl sulfoxide (Catalog No. D807976) were sourced from Shanghai Maclin Biochemical Technology Co., Ltd. (Shanghai, China). potassium carbonate (Catalog No. A17026), tetrahydrofuran (Catalog No. W310137), methanol (Catalog No. A04002925) were sourced from Shanghai Titan Scientific Technology Co., Ltd. (Shanghai, China). Dulbecco's Modified Eagle's Medium (Catalog No. KGL1202-500) and phosphate-buffered saline (Catalog No. KGL2206-500) were obtained from Jiangsu Kaiji Biotechnology Co., Ltd. (Jiangsu, China). Additionally, Thiazoyl blue tetrazolium bromide (MTT) (Catalog No: L11939.03) was purchased from Thermo Fisher Scientific (Waltham, MA, USA). Nuclear magnetic resonance (NMR) spectroscopy was performed using a Bruker 600 MHz NMR spectrometer (AVANCE NEO 600MHz, Bruker Corporation, Fällanden, Switzerland). LC-MS analyses were conducted on an ISQEM-ESI system from Thermo Fisher Scientific. UV-Vis absorption spectra were recorded using an Agilent Cary 60 spectrometer (Agilent Technologies Inc., Santa Clara, CA, USA), while fluorescence spectra were measured with a Lumina fluorescence spectrophotometer from Thermo Fisher Scientific. Cellular fluorescence imaging was conducted using a Carl Zeiss LSM800 confocal laser scanning microscope (Carl Zeiss AG, Oberkochen, German).

2.2 Synthesis

The synthetic pathway for the probe **DCMOS-N** is illustrated in Fig. 2, with detailed synthetic procedures provided in the synthesis section of the Supporting Infor-

mation. The chemical structures of all intermediates and the final probe were thoroughly characterized using ^1H NMR, ^{13}C NMR, and LC-MS (**Supplementary Material-Supporting Information, Supplementary Figs. 1–12**).

2.3 Design of the Probe DCMOS-N

To overcome the challenges of short emission wavelengths and limited Stokes shifts in probe molecules, dicyanomethylene-4H-pyran (**DCM**) was chosen as the fluorophore due to its excellent photochemical and chemical stability, as well as its tunable emission properties. **DCM** was modified through a Knoevenagel condensation reaction, extending its conjugated system and resulting in the formation of **DCMOS**, which shifted the fluorescence emission into the near-infrared region (with a maximum emission wavelength of 651 nm). Additionally, DNBS was introduced as a recognition unit for biothiols, yielding the NIR fluorescent probe by linking the fluorophore **DCMOS** to the strong electron-withdrawing DNBS group via a sulfonic ester linker.

2.4 Fluorescence Detection of Probe DCMOS-N

The general method for spectroscopic analysis is outlined below unless stated otherwise. Stock solutions of the **DCMOS** fluorophore and probe **DCMOS-N** were prepared at a concentration of 10 mM in DMSO. For testing, a THF/PBS buffer solution was used. The spectroscopic properties of **DCMOS-N** were analyzed at a concentration of 10 $\mu\text{mol/L}$. The interaction between probe **DCMOS-N** and biothiols was evaluated in a THF/PBS buffer mixture ($v/v = 4/6$, $\text{pH} = 7.4$). The mixture was then transferred to a quartz cuvette with a 1 cm path length for fluorescence measurements, using an excitation wavelength of 480 nm and an emission wavelength of 651 nm, with both slit widths set to 10 nm.

2.5 Cell Viability Assay

HeLa cells (CL-0101) were kindly provided by Wuhan Pricella Biotechnology Co., Ltd. (Wuhan, China) and cultured in DMEM supplemented with 10% fetal bovine serum and 1% penicillin-streptomycin, maintained in a CO_2 incubator at 37°C with 5% CO_2 and 95% air. The cell line was validated by STR profiling and tested negative for mycoplasma. The cytotoxicity of **DCMOS** and **DCMOS-N** was evaluated using the Methylthiazolyldiphenyl-tetrazolium bromide (MTT) assay. A sterilized 96-well plate was used, with each well containing 100 μL of HeLa cell suspension at a density of 5×10^3 cells per well. The cells were allowed to adhere for 24 hours before being treated with **DCMOS** and **DCMOS-N** at concentrations of 1, 2.5, 5, 7.5, 10, 15, 20, and 30 $\mu\text{mol/L}$. They were then incubated at 37°C in 5% CO_2 for an additional 24 hours. Following incubation, the medium was removed, and 100 μL of DMSO was added to each well to dissolve the formazan crystals with shaking. Absorbance

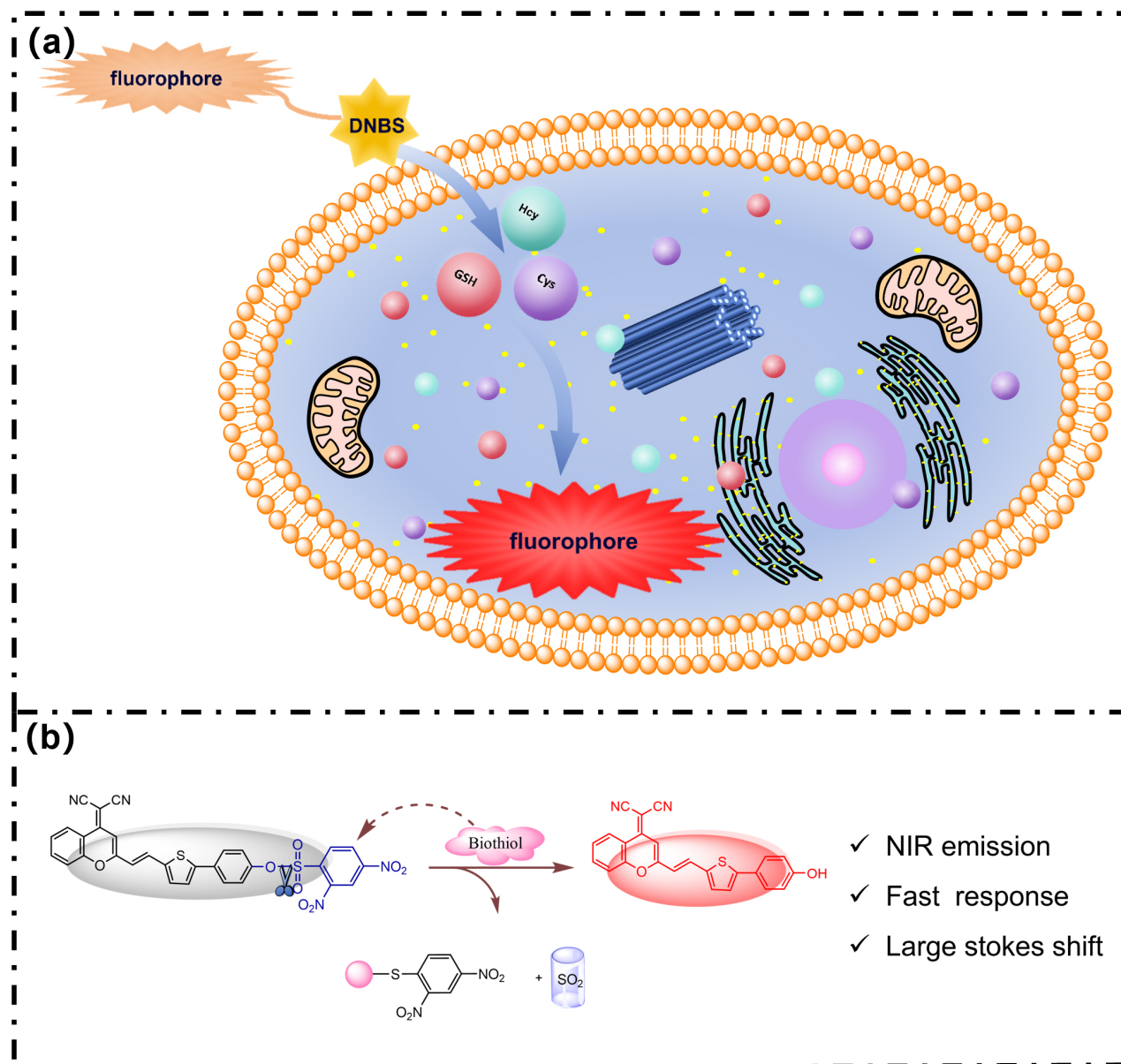


Fig. 1. Mechanistic insights into DCMOS-N fluorescent probe for cellular biothiol detection. (a) Schematic diagram of the fluorescent probe for detecting biothiols in living cells. (b) Design and response mechanism of **DCMOS-N** to biothiols. DNBS, 2,4-dinitrobenzenesulfonyl; GSH, glutathione; Cys, cysteine; Hcy, homocysteine; NIR, near-infrared; DCMOS-N, (E)-4-(5-(2-(4-(dicyanomethylene)-4H-chromen-2-yl)vinyl)thiophen-2-yl)phenyl 2,4-dinitrobenzenesulfonate.

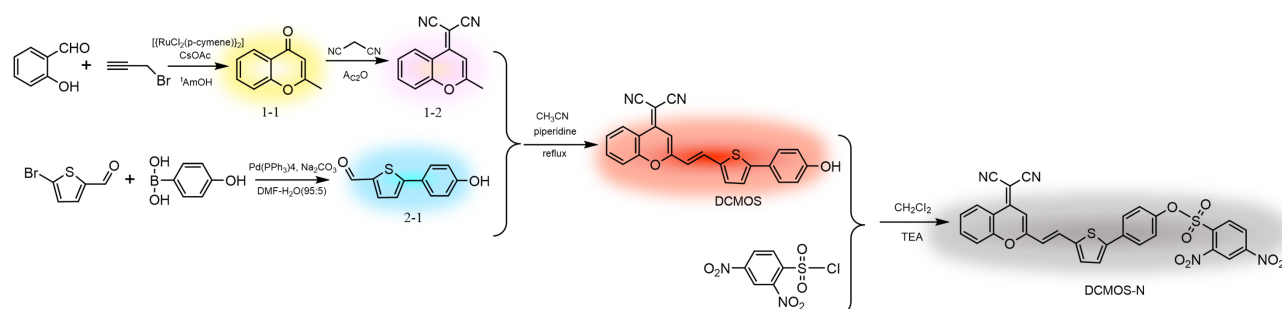


Fig. 2. Synthetic route for DCMOS-N.

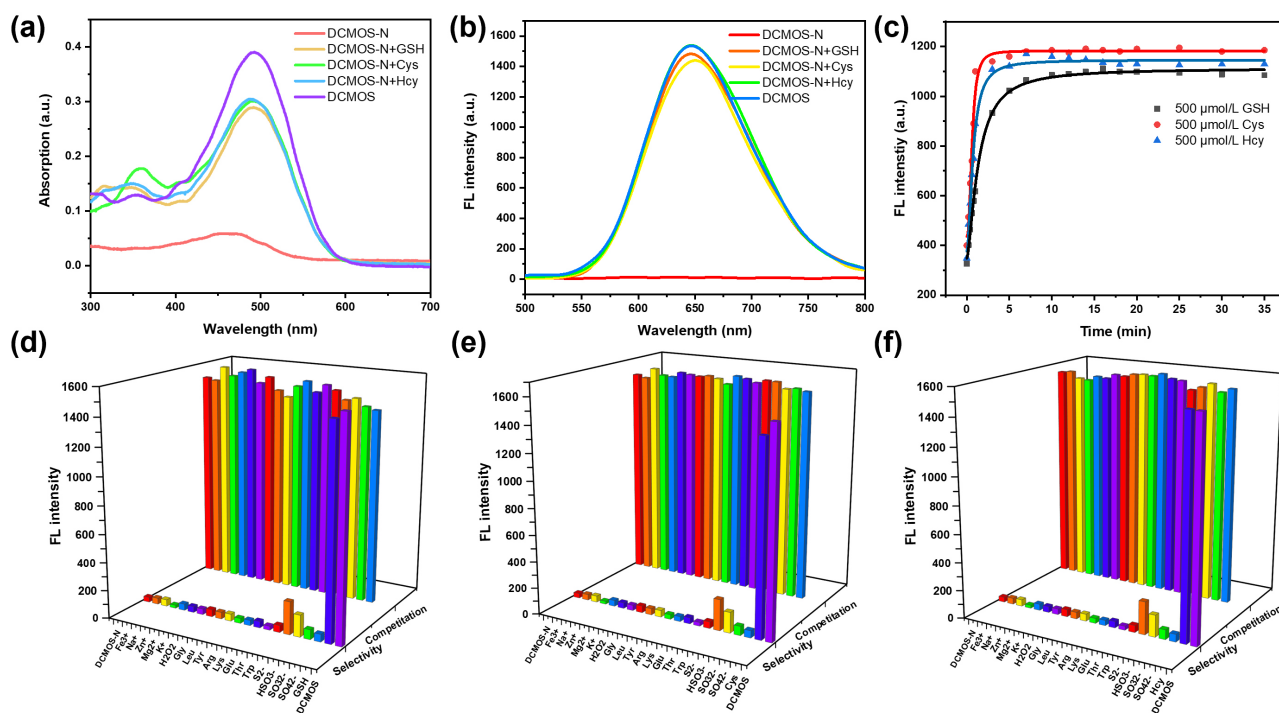


Fig. 3. Investigation of the characteristics of the probe DCMOS-N. Absorption (a) and fluorescence spectra (b) of probe DCMOS-N (10 $\mu\text{mol/L}$) with biothiols in THF/PBS (4/6, v/v, 10 $\mu\text{mol/L}$, pH 7.4). (c) The reaction kinetics of DCMOS-N with biothiols. (d–f) The fluorescence selectivity and competitive analysis of DCMOS-N (10 $\mu\text{mol/L}$) upon the addition of various analytes (Fe³⁺, Na⁺, Zn²⁺, Mg²⁺, K⁺, H₂O₂, S²⁻, HSO₃⁻, SO₃²⁻, and SO₄²⁻, glycine (Gly), leucine (Leu), arginine (Arg), tyrosine (Tyr), glutamic acid (Glu), threonine (Thr), tryptophan (Trp), GSH, Cys and Hcy each at 500 $\mu\text{mol/L}$). (λ_{ex} = 480 nm). FL, fluorescence.

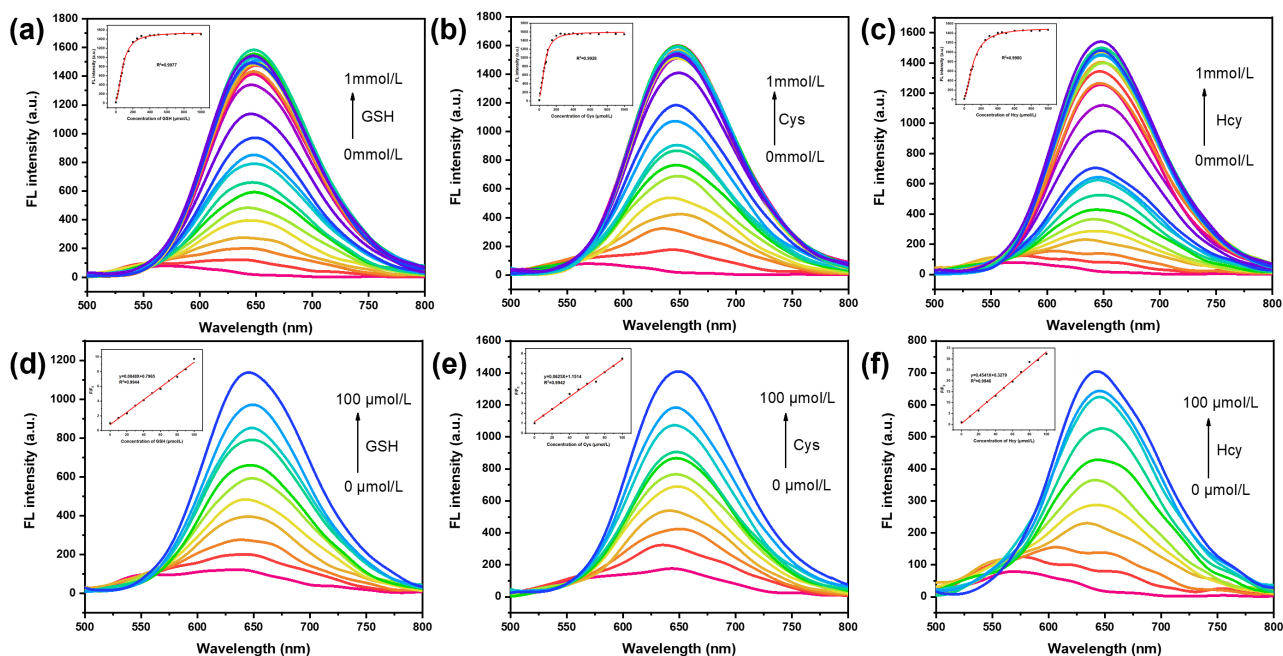


Fig. 4. Fluorescence spectra of probe DCMOS-N in response to biothiols of different concentrations. Fluorescence spectra of probe DCMOS-N (10 $\mu\text{mol/L}$) in response to three biothiols: GSH (a), Cys (b), and Hcy (c) at varying concentrations (0–1 mmol/L). Insets in (a–c): Fluorescence intensity of probe DCMOS-N (10 $\mu\text{mol/L}$) at different biothiol concentrations (0–1 mmol/L). Insets in (d–f): Linear relationship between the fluorescence intensity ratio (F/F_0) and biothiol concentration (0–100 $\mu\text{mol/L}$). (λ_{ex} = 480 nm). “↑” indicates that the fluorescence intensity shows a gradually increasing trend with the increase of concentration.

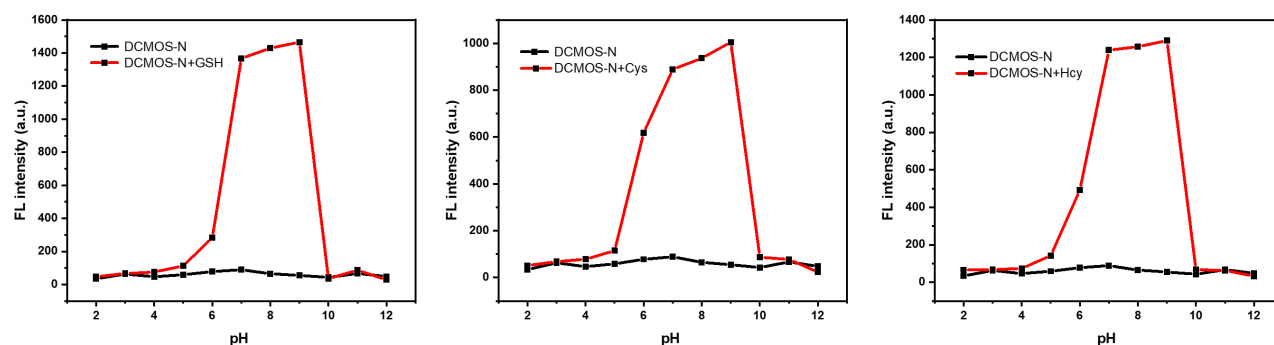


Fig. 5. The fluorescence intensity of probe DCMOS-N (10 $\mu\text{mol/L}$) in different pH solutions after adding GSH, Cys and Hcy (10 $\mu\text{mol/L}$) ($\lambda_{\text{ex}} = 480 \text{ nm}$).

was measured at 490 nm using a Thermo Fisher Varioskan Flash multimode microplate reader (Thermo Fisher Scientific). Cell viability at 0 $\mu\text{mol/L}$ probe concentration was set to 100%. The percentage of cell viability was calculated using the following formula: Cell viability (%) = (Mean optical density of the sample \times 100)/(Mean optical density of the control group).

2.6 Fluorescence Imaging in Living Cells

Cell imaging at varying concentration gradients was performed by treating HeLa cells with 20 $\mu\text{mol/L}$ DCMOS-N. Fluorescence images were acquired using a Carl Zeiss LSM800 confocal laser scanning microscope. Imaging parameters included a $\times 63$ objective, 12% laser intensity, a 40 μm pinhole size, and a voltage gain of 750 V. The excitation wavelength was set at 488 nm, with emission captured in the 600–700 nm range.

3. Results and Discussion

3.1 Optical Properties of Probe DCMOS-N for Biothiols

To evaluate the effectiveness of DCMOS-N, preliminary experiments were conducted to determine the optimal conditions for detecting biothiols (GSH, Cys, Hcy). THF/PBS (4/6, v/v, 10 $\mu\text{mol/L}$, pH 7.4) was identified as the most suitable testing environment (Supplementary Figs. 13,14). Subsequently, the absorption and fluorescence spectra of probe DCMOS-N (10 $\mu\text{mol/L}$) were recorded before and after interaction with biothiols (500 $\mu\text{mol/L}$). As illustrated in Fig. 3a, the unreacted probe DCMOS-N exhibited a weak absorption peak at 470 nm, which disappeared upon the addition of biothiols, while a new peak emerged at 493 nm, closely matching the absorption peak of DCMOS. Fig. 3b illustrates that initially, probe DCMOS-N displayed minimal fluorescence. Notably, a significant fluorescence enhancement at 651 nm was observed upon the addition of biothiols, indicating a structural change in DCMOS-N upon reaction with biothiols. Furthermore, kinetic studies of DCMOS-N with GSH, Cys, and Hcy at 651 nm revealed peak fluorescence intensities at approximately 2, 5, and 7 minutes, with significant enhancements

of 10-, 7-, and 14.5-fold, respectively Fig. 3c. Additionally, the interaction product DCMOS, formed from the reaction between DCMOS-N and biothiols, exhibited a substantial Stokes shift of 151 nm, making it highly advantageous for bioimaging applications (Supplementary Fig. 15).

Selectivity and anti-interference capabilities are crucial for evaluating the effectiveness of a fluorescent probe. To assess these properties, DCMOS-N was tested against various ions, including Fe^{3+} , Na^+ , Zn^{2+} , Mg^{2+} , K^+ , H_2O_2 , S^{2-} , HSO_3^- , SO_3^{2-} , and SO_4^{2-} , as well as amino acids such as glycine (Gly), leucine (Leu), arginine (Arg), tyrosine (Tyr), glutamic acid (Glu), threonine (Thr), tryptophan (Trp), alongside biothiols (Cys, Hcy, and GSH). As illustrated in Fig. 3d–f, a significant fluorescence enhancement was observed only in the biothiol test groups, indicating strong selectivity. Additionally, the anti-interference performance of DCMOS-N was evaluated, demonstrating that the presence of other potential interferents had no impact on its ability to detect biothiols. These findings confirm that DCMOS-N exhibits high selectivity and strong anti-interference properties, highlighting its potential for biothiol detection in live-cell bioimaging.

To thoroughly investigate the interaction between DCMOS-N and biothiols, a concentration titration experiment was conducted with biothiol concentrations ranging from 0 to 1 mmol/L (Fig. 4). First, DCMOS-N exhibited negligible fluorescence emission; however, a gradual increase in fluorescence intensity was observed as the biothiol concentration increased (Fig. 4a–c). The fluorescence intensity at 651 nm was measured and recorded, and the resulting data were used to generate response curves (Fig. 4a–c, inset). A strong linear correlation was observed within the concentration range of 0 to 100 $\mu\text{mol/L}$, with R^2 values of 0.9944 for GSH, 0.9942 for Cys, and 0.9946 for Hcy (Fig. 4d–f, inset), enabling the quantitative analysis of biothiol concentrations in biological systems. Additionally, the limits of detection (LOD) for GSH, Cys, and Hcy were calculated to be 0.142, 0.129, and 0.143 $\mu\text{mol/L}$, respectively (Supplementary Figs. 16–18). Moreover, a comparative analysis of recently developed fluorescent probes

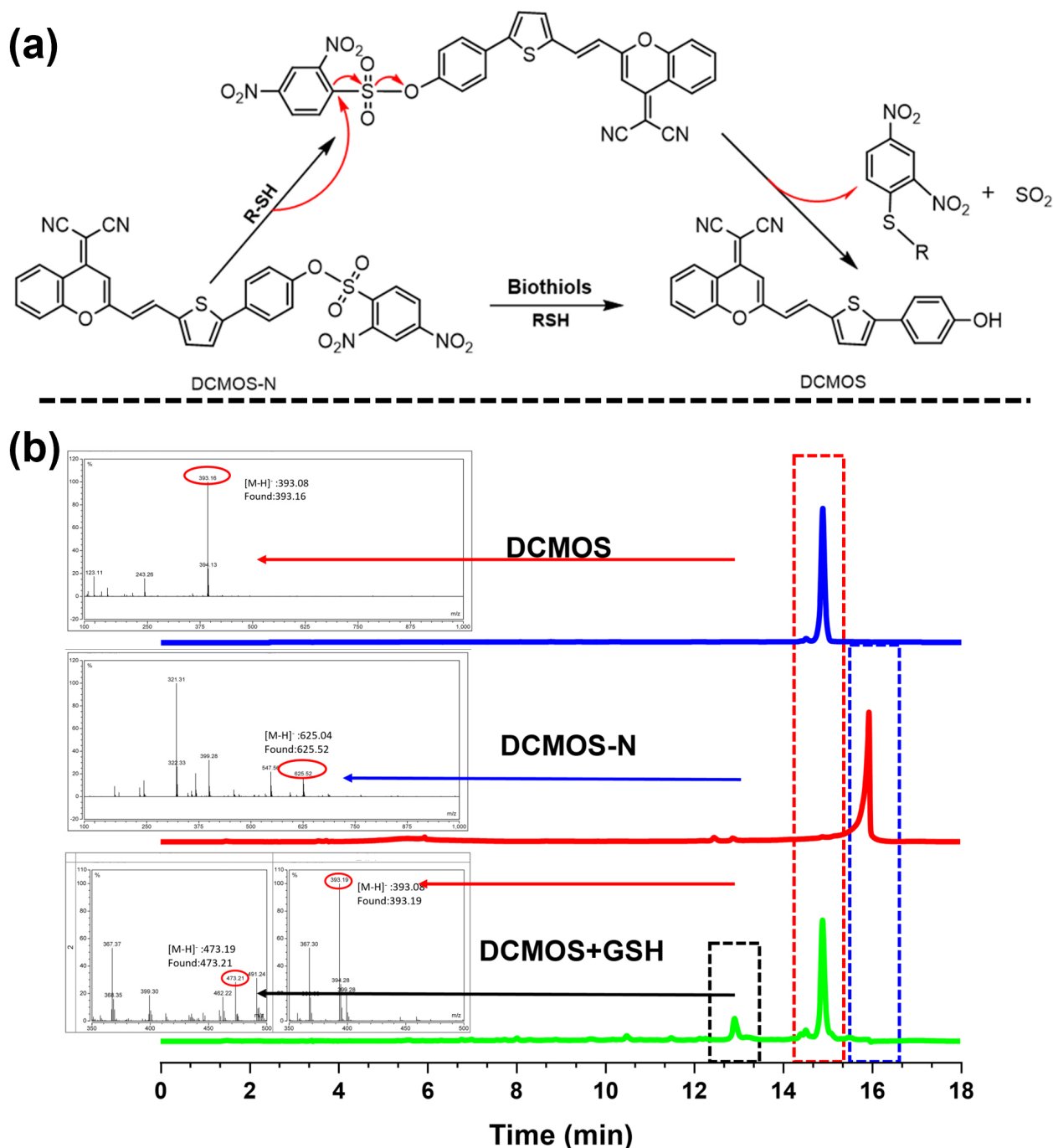


Fig. 6. Mechanistic study of the probe DCMOS-N for biothiols. (a) Proposed mechanism of DCMOS-N for biothiol recognition. (b) LC-MS analysis of DCMOS-N (10 $\mu\text{mol/L}$) after the addition of GSH (10 $\mu\text{mol/L}$).

employing 2,4-dinitrobenzenesulfonyl (DNBS) as a recognition moiety, including LOD, media, and applications, is presented in **Supplementary Table 1**. The probe DCMOS-N has advantages in terms of LOD, with higher sensitivity. These findings confirm that DCMOS-N can sensitively detect biothiols, facilitating fluorescence-based detection even at low concentrations.

The photophysical properties of DCMOS-N and its cleavage product DCMOS were characterized. DCMOS-N exhibited a quantum yield (QY) of 27.4%, while DC-

MOS showed a significantly higher QY of 58.2% (2.1-fold enhancement), indicating enhanced fluorescence efficiency for sensitive detection. The extinction coefficient (ϵ) of DCMOS-N was $5500 \text{ M}^{-1}\cdot\text{cm}^{-1}$, versus $37,300 \text{ M}^{-1}\cdot\text{cm}^{-1}$ for DCMOS, suggesting improved light absorption and signal-to-noise ratio. These superior photophysical properties of DCMOS, make it particularly suitable for high-contrast bioimaging (**Supplementary Fig. 19**).

The optimal pH range for probe DCMOS-N (10 $\mu\text{mol/L}$) in detecting biothiols (100 $\mu\text{mol/L}$) was deter-

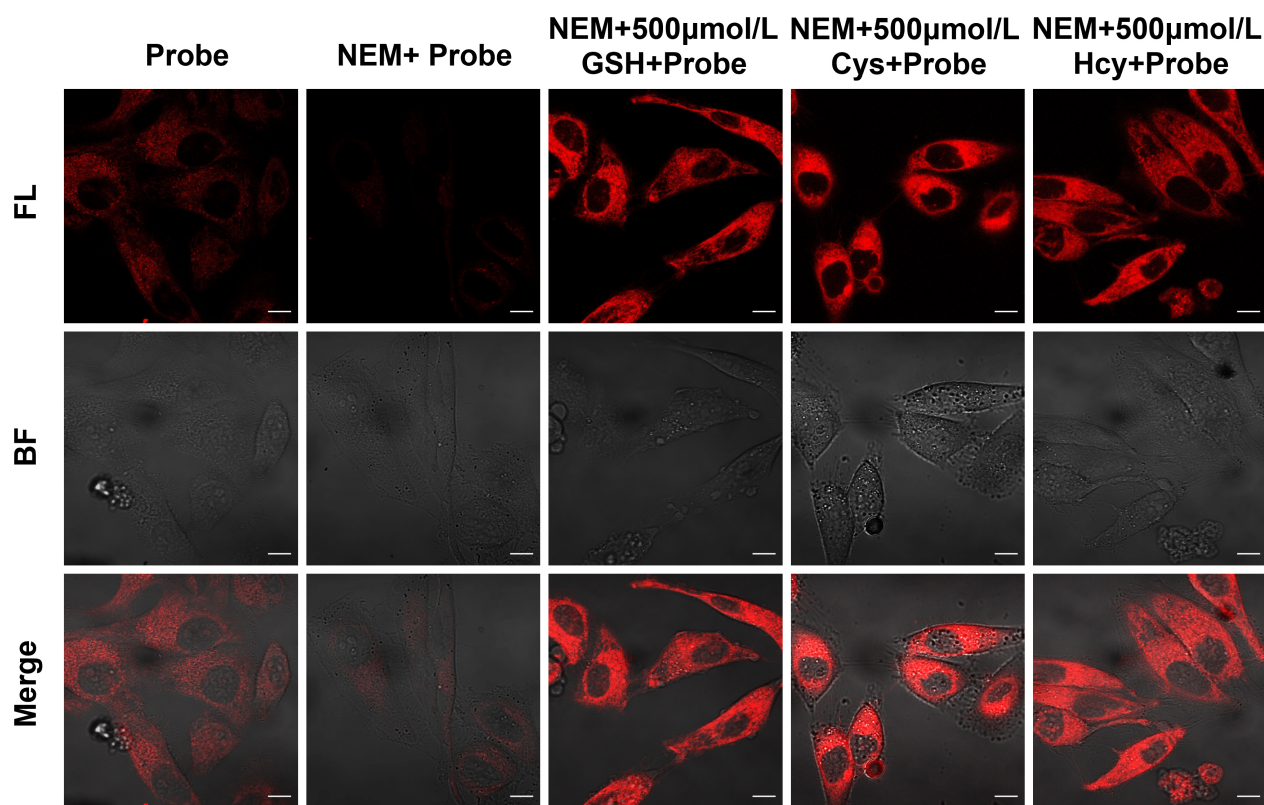


Fig. 7. Confocal fluorescence images of endogenous and exogenous biothiols in living HeLa cells. First column: HeLa cells were incubated with probe **DCMOS-N** (20 $\mu\text{mol/L}$); second column: HeLa cells were incubated with NEM (200 $\mu\text{mol/L}$) and **DCMOS-N** (20 $\mu\text{mol/L}$); third column: NEM-pretreated HeLa cells incubated with GSH (500 $\mu\text{mol/L}$) and **DCMOS-N** (20 $\mu\text{mol/L}$); forth column: NEM-pretreated HeLa cells incubated with Cys (500 $\mu\text{mol/L}$) and **DCMOS-N** (20 $\mu\text{mol/L}$); fifth column: NEM-pretreated HeLa cells incubated with Hcy (500 $\mu\text{mol/L}$) and **DCMOS-N** (20 $\mu\text{mol/L}$). FL, fluorescence imaging; BF, bright field imaging. $\lambda_{\text{ex}} = 488 \text{ nm}$, $\lambda_{\text{em}} = 600\text{--}700 \text{ nm}$. Imaging scale bar = 10 μm . NEM, N-ethylmaleimide.

mined based on the physiological pH conditions of living organisms. The fluorescence response of **DCMOS-N** was analyzed before and after interaction with biothiols across a pH range of 2 to 12. As illustrated in Fig. 5, the fluorescence intensity of **DCMOS-N** at 651 nm remained relatively stable under varying pH conditions. However, upon the addition of biothiols, a significant fluorescence increase was observed within the pH range of 5 to 7. The intensity showed a slight decline in weakly alkaline conditions but remained stable between pH 7 and 9. Combined with the pH-dependent test results of **DCMOS** (Supplementary Fig. 20). Given that most organisms maintain a physiological pH between 7.35 and 7.45, these findings indicate that probe **DCMOS-N** is well-suited for detecting biothiols within biological systems.

3.2 Proposed Response Mechanism of **DCMOS-N** to Biothiols

The proposed mechanism by which **DCMOS-N** recognizes biothiols is illustrated in Fig. 6a. Previous study has shown that the sulfhydryl group ($-\text{SH}$) in biothiols can undergo a nucleophilic substitution reaction with the DNBS

group in the probe [21]. Specifically, the $-\text{SH}$ group of biothiols attacks the benzene ring within the DNBS moiety, triggering a nucleophilic substitution reaction that ultimately releases SO_2 and generates the NIR-emitting dye, **DCMOS**. To confirm this mechanism, the reaction mixture of **DCMOS-N** and GSH was analyzed using LC-MS. As shown in Fig. 6b, the chromatographic peaks in the high-performance liquid spectroscopy spectra for **DCMOS** and **DCMOS-N** appeared at 14.91 and 15.95 minutes, respectively. However, after allowing **DCMOS-N** to react with GSH for 10 minutes, two new peaks emerged, corresponding to **DCMOS** (14.91 minutes) and another reaction product (12.92 minutes), while the peak for **DCMOS-N** disappeared. In the mass spectrometry analysis, two new peaks were observed at m/z 393.19 and 473.21 (Supplementary Fig. 21), corresponding to the NIR fluorophore **DCMOS** and the substitution product, respectively. These results provide strong evidence that the interaction between biothiols and the DNBS group of **DCMOS-N** involves a nucleophilic attack, leading to the formation of the NIR-emitting product **DCMOS**. This detailed mechanistic insight further validates the probe's effectiveness in detecting biothiols.

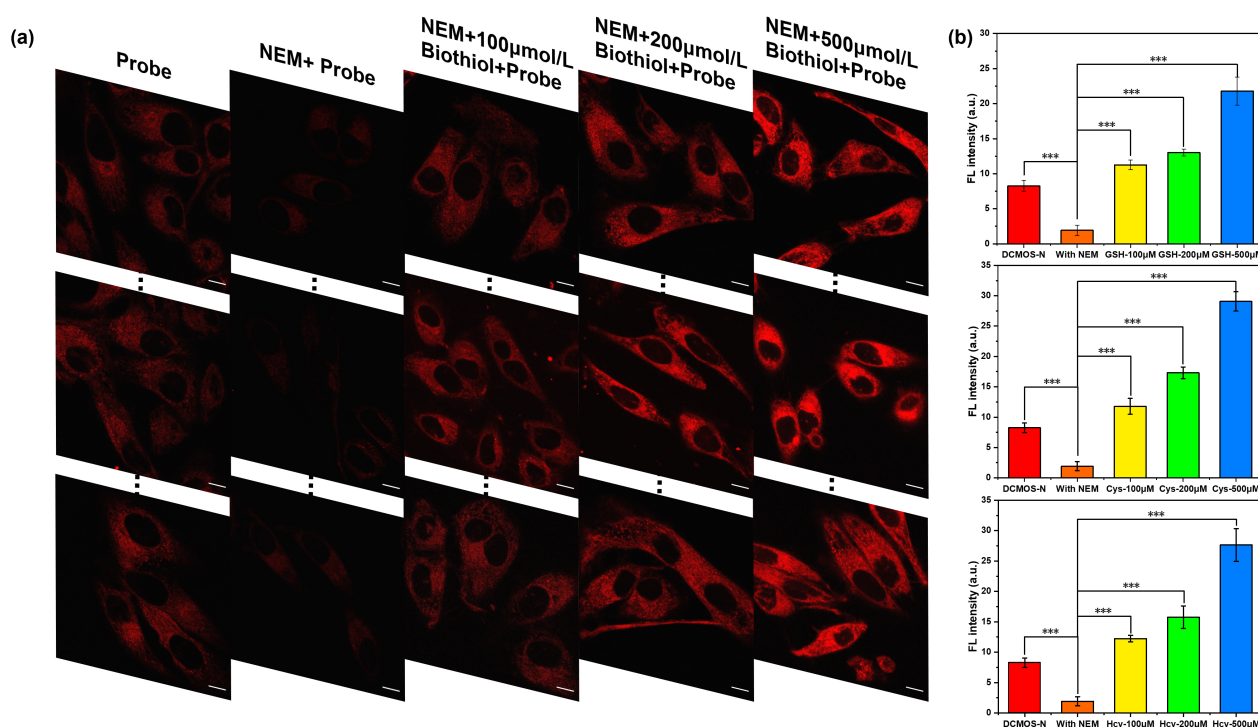


Fig. 8. Bio-imaging applications of DCMOS-N for detecting various concentrations (100 µmol/L, 200 µmol/L, 500 µmol/L) biothiols in living cells. (a) Confocal fluorescence images of different concentrations biothiols in living HeLa cells. (b) The fluorescence intensity variation with different concentrations biothiols. The data were analysed by ImageJ software (2.0, National Institutes of Health, Maryland, MD, United States). First line: GSH; second line: Cys; third line: Hcy. $\lambda_{\text{ex}} = 488 \text{ nm}$, $\lambda_{\text{em}} = 600\text{--}700 \text{ nm}$. Imaging scale bar = 10 µm. Significance was determined by the *t*-test (***, $p < 0.001$).

3.3 Fluorescent Imaging in Living Cells

Encouraged by the excellent fluorescence response of **DCMOS-N** toward biothiols, further studies were conducted to explore its potential for monitoring biothiols in living HeLa cells. Before proceeding with real-time cellular imaging, an MTT assay was performed to assess the cytotoxicity of **DCMOS-N**. As illustrated in **Supplementary Figs. 22–24**, HeLa, U2OS, and Jurkat cell viability remained above 80% after a 24-hour incubation with 30 µmol/L **DCMOS-N**, confirming its minimal cytotoxicity and suitability for live-cell imaging. Subsequently, the application of **DCMOS-N** for detecting biothiols in living HeLa cells was investigated using confocal microscopy. As illustrated in Fig. 7, a distinct red fluorescence signal was observed after a 30-minute incubation with the probe, indicating the presence of endogenous biothiols. However, when cells were pretreated with the well-known biothiol scavenger N-ethylmaleimide (NEM) for 30 minutes before exposure to **DCMOS-N**, virtually no red fluorescence was observed. To verify the capability of **DCMOS-N** for detecting exogenous biothiols, cells were first treated with NEM to deplete endogenous thiols. A strong red fluorescence signal was then detected after subsequent incubation with GSH and **DCMOS-N** for 30 minutes. Similar fluorescence responses were observed when Cys and Hcy were in-

troduced. Moreover, no changes in cell morphology were noted throughout the experiment. These findings confirm that the probe is non-toxic and can effectively detect both endogenous and exogenous biothiols in living HeLa cells. Fluorescence imaging of cells treated with varying concentrations of biothiols and the corresponding quantitative analysis of fluorescence intensity are provided in **Supplementary Figs. 25–30**.

Additionally, experiments were conducted to demonstrate that **DCMOS-N** could be used to measure actual intracellular biothiol concentrations (Fig. 8). Fluorescence imaging of glutathione and cysteine at varying concentrations are shown in **Supplementary Figs. 31–36**, respectively. Cells were incubated with varying concentrations of biothiols for 30 minutes, followed by fluorescence imaging. The results showed a gradual increase in fluorescence intensity as biothiol concentration increased, consistent with observations in buffer solutions. These findings confirm that probe **DCMOS-N** is a promising tool for imaging biothiols in living cells.

4. Conclusion

In summary, an NIR fluorescent probe, **DCMOS-N**, was developed for biothiol detection, utilizing the 2,4-dinitrobenzenesulfonyl group as the recognition unit.

DCMOS-N exhibited excellent sensitivity and selectivity toward biothiols, with a rapid response time of just 2 minutes and a detection limit as low as 0.129 $\mu\text{mol/L}$. Notably, **DCMOS-N** effectively monitored endogenous biothiols in living HeLa cells. This capability arises from a nucleophilic substitution reaction in which the sulfhydryl (-SH) group of biothiols attacks the benzene ring of the 2,4-dinitrobenzenesulfonyl group in **DCMOS-N**, leading to the release of the fluorophore **DCMOS** and the generation of an NIR fluorescence signal. The successful development of **DCMOS-N** provides a promising platform for designing fluorescent probes targeting biothiols, with broad potential applications in biochemical research. We hope that **DCMOS-N** could be conducted *in vivo* to evaluate its biocompatibility and performance in more complex biological environments.

Availability of Data and Materials

The datasets used and/or analyzed during the current study are available from the corresponding author on reasonable request.

Author Contributions

XL and SM conceived and designed the research. XL and GL conducted the experiments. XL and RY analyzed the data. YM provided help and advice on the design. XL and SM wrote the manuscript. GL, RY, and YM were involved in both drafting the manuscript and critically reviewing it for important intellectual content. All authors contributed to editorial changes in the manuscript. All authors read and approved the final manuscript. All authors have participated sufficiently in the work and agreed to be accountable for all aspects of the work.

Ethics Approval and Consent to Participate

Not applicable.

Acknowledgment

We would like to express our gratitude to all those who helped us during the writing of this manuscript.

Funding

This work was supported by the Science and Technology Plan Project of Xi'an (21NYF0057); Science and Technology Plan Project of Weiyang District (202114).

Conflict of Interest

The authors declare no conflict of interest.

Supplementary Material

Supplementary material associated with this article can be found, in the online version, at <https://doi.org/10.31083/FBL37240>.

References

- [1] Zhu Y, Pan H, Song Y, Jing C, Gan J-A, Zhang J. Mitochondria-targeted fluorescent probe for rapid detection of thiols and its application in bioimaging. *Dyes and Pigments*. 2021; 191: 109376. <https://doi.org/https://doi.org/10.1016/j.dyepig.2021.109376>.
- [2] Yue Y, Huo F, Ning P, Zhang Y, Chao J, Meng X, *et al.* Dual-Site Fluorescent Probe for Visualizing the Metabolism of Cys in Living Cells. *Journal of the American Chemical Society*. 2017; 139: 3181–3185. <https://doi.org/10.1021/jacs.6b12845>.
- [3] Zhou M, Lin Y, Bai T, Ye T, Zeng Y, Li L, *et al.* An activated near-infrared fluorescent probe with large Stokes shift for discrimination of bio-thiols. *Sensors and Actuators B: Chemical*. 2024; 414: 135994. <https://doi.org/https://doi.org/10.1016/j.snb.2024.135994>.
- [4] Yang Y, Liu X, Xi D, Zhang Y, Gao X, Xu K, *et al.* Precision Imaging of Biothiols in Live Cells and Treatment Evaluation during the Development of Liver Injury via a Near-Infrared Fluorescent Probe. *Chemical & Biomedical Imaging*. 2024; 3: 169–179. <https://doi.org/10.1021/cbmi.4c00048>.
- [5] Wang L, Wang J, Xia S, Wang X, Yu Y, Zhou H, *et al.* A FRET-based near-infrared ratiometric fluorescent probe for detection of mitochondria biothiol. *Talanta*. 2020; 219: 121296. <https://doi.org/10.1016/j.talanta.2020.121296>.
- [6] Lu W-Y, Li H-J, Wu Y-C. Assessment of environmental and biological stress using mitochondria-targeted red-emitting and near-infrared fluorescent probes for biothiol analysis: a review. *Environmental Chemistry Letters*. 2024; 22: 3135–3169. <https://doi.org/10.1007/s10311-024-01761-z>.
- [7] Wang Y, Li M, Yu H, Chen Y, Cui M, Ji M, *et al.* A Near-Infrared Fluorescent Dye with Tunable Emission Wavelength and Stokes Shift as a High-Sensitivity Cysteine Nanoprobe for Monitoring Ischemic Stroke. *ACS Nano*. 2024; 18: 15978–15990. <https://doi.org/10.1021/acsnano.4c04211>.
- [8] Yang Y, Zhou T, Jin M, Zhou K, Liu D, Li X, *et al.* Thiol-Chromene “Click” Reaction Triggered Self-Immulative for NIR Visualization of Thiol Flux in Physiology and Pathology of Living Cells and Mice. *Journal of the American Chemical Society*. 2020; 142: 1614–1620. <https://doi.org/10.1021/jacs.9b12629>.
- [9] Chen W, Luo N, Zhang Y, Tang LJ, Wang F, Jiang JH. An activatable near-infrared fluorescent probe facilitated high-contrast lipophagic imaging in live cells. *Chemical Communications (Cambridge, England)*. 2021; 57: 8664–8667. <https://doi.org/10.1039/d1cc03259c>.
- [10] Hu L, Lin Y, Wang P, Zhang H, Liu M, Mo S. A rhodamine derivative probe for highly selective detection of Cu(II). *Frontiers in Bioscience (Landmark Edition)*. 2022; 27: 28. <https://doi.org/10.31083/j.fbl2701028>.
- [11] Kang Y-F, Niu L-Y, Yang Q-Z. Fluorescent probes for detection of biothiols based on “aromatic nucleophilic substitution-rearrangement” mechanism. *Chinese Chemical Letters*. 2019; 30: 1791–1798. <https://doi.org/https://doi.org/10.1016/j.ccllet.2019.08.013>.
- [12] Yu L, Xie M, Chen M, Yang H, Chen L, Xing P, *et al.* An ortho-activation strategy to develop NIR fluorescent probe for rapid imaging of biothiols in vivo. *Talanta*. 2024; 266: 125110. <https://doi.org/10.1016/j.talanta.2023.125110>.
- [13] Gao Z, Yang H, Ran L, Zhang D, Ren Y, Wang F, *et al.* Water-Soluble Dual-Channel Fluorescent Probe for Sensitive Detection of Biothiols In Vitro and In Vivo. *ACS Applied Bio Materials*. 2023; 6: 5828–5835. <https://doi.org/10.1021/acsbm.3c00928>.
- [14] Yang Y, Ma M, Shen L, An J, Kim E, Liu H, *et al.* A Fluorescent Probe for Investigating the Role of Biothiols in Signaling Pathways Associated with Cerebral Ischemia-Reperfusion Injury. *Angewandte Chemie (International Ed. in English)*. 2023; 62: e202310408. <https://doi.org/10.1002/anie.202310408>.

- [15] Wu Y, Guo X, Ma X, Zhu Y, Liu Y, Zeng H. Novel near-infrared frequency up-conversion luminescence probe for monitoring biothiols in vitro and in vivo. *Sensors and Actuators B: Chemical*. 2023; 385: 133705. <https://doi.org/10.1016/j.snb.2023.133705>.
- [16] Chen Z, Wang B, Liang Y, Shi L, Cen X, Zheng L, *et al.* Near-Infrared Fluorescent and Photoacoustic Dual-Mode Probe for Highly Sensitive and Selective Imaging of Cysteine *In Vivo*. *Analytical Chemistry*. 2022; 94: 10737–10744. <https://doi.org/10.1021/acs.analchem.2c01372>.
- [17] Zheng C, Zhou X, Wang H, Ji M, Wang P. A novel ratiometric fluorescent probe for the detection and imaging of cysteine in living cells. *Bioorganic Chemistry*. 2022; 127: 106003. <https://doi.org/10.1016/j.bioorg.2022.106003>.
- [18] Wu Z, Zhang D, Ma H, Wang E, Wang F, Ren J. Near-infrared colorimetric and ratiometric fluorescent probe for dual-channel imaging of mitochondria and cysteine in the oxidative stress model. *Chemical Engineering Journal*. 2023; 475: 146397. <https://doi.org/10.1016/j.cej.2023.146397>.
- [19] Li N, Wang T, Wang N, Fan M, Cui X. A Substituted-Rhodamine-Based Reversible Fluorescent Probe for In Vivo Quantification of Glutathione. *Angewandte Chemie (International Ed. in English)*. 2023; 62: e202217326. <https://doi.org/10.1002/anie.202217326>.
- [20] Ma H, Luo Z, Ding J, Zhang D, Wang F, Yu H, *et al.* Fluorescent probe for tumor imaging and prognostic assessment via multi-response to biothiols, viscosity, and pH values. *Sensors and Actuators B: Chemical*. 2025; 424: 136926. <https://doi.org/10.1016/j.snb.2024.136926>.
- [21] Yang L, Xiong H, Su Y, Tian H, Liu X, Song X. A red-emitting water-soluble fluorescent probe for biothiol detection with a large Stokes shift. *Chinese Chemical Letters*. 2019; 30: 563–565. <https://doi.org/10.1016/j.cclet.2018.12.017>.